THE ASTROPHYSICAL JOURNAL, 468:L119–L122, 1996 September 10

THE NATURE OF THE MOLECULAR LINE WING EMISSION IN THE ROSETTE MOLECULAR COMPLEX

N. SCHNEIDER, J. STUTZKI, AND G. WINNEWISSER
I. Physikalisches Institut, Universität zu Köln, Zülpicher Straße 77, D-50937 Köln, Germany

AND

L. BLITZ
Department of Astronomy, University of Maryland, College Park, MD 20742-2421
Received 1996 January 31; accepted 1996 June 28

ABSTRACT

We present ^{12}CO and ^{13}CO $J = 3 \rightarrow 2$ and $J = 2 \rightarrow 1$ observations of the Rosette Molecular Complex. The observations show that broad line wings, originally observed in CO $J = 1 \rightarrow 0$, also exist in the higher J lines in high signal-to-noise ratio spectra toward individual positions and in positionally averaged spectra. We show that the wing emission can be explained by the superposition of individual high- and low-velocity clumps, some of which are spatially resolved at high angular resolution, and at least two embedded outflow sources. Our results call in question an earlier interpretation of this weak line wing emission as originating from a low-density, ubiquitous, molecular interclump gas. A multiline analysis implies that the wing emission originates in gas with densities comparable to the density of the bulk emission. We note that the physical conditions derived from this relatively simple single-component excitation analysis do not give a fully consistent picture of these clumps, leaving any conclusion on their dynamical state and evolution rather speculative.

Subject headings: ISM: clouds — ISM: individual (Rosette Molecular Complex) — ISM: molecules — ISM: structure — line: profiles — radio lines: general

1. INTRODUCTION

Molecular clouds exhibit a highly inhomogeneous density structure on all size scales. This is revealed by detailed mapping of numerous Galactic sources in molecular emission lines (see, e.g., Stutzki 1993 for a review). The relatively sharp positional confinement of density enhancements (clumps) suggests that they are embedded in a lower density substrate, the "interclump gas." From CO and [C II] observations, the density contrast between these two phases in warm dense clouds appears to be at least a few times 10 (Stutzki et al. 1988; Stutzki & Güsten 1990), whereas it is significantly smaller in dark clouds (Perault, Falgarone, & Puget 1985).

The interclump gas plays an important role in the dynamic evolution of a cloud. Gravitionally unbound clumps may be confined by the pressure of warm interclump gas (Bertoldi & McKee 1992). Its composition is subject to ongoing research, and the Rosette Molecular Complex (RMC) has been a prime object of these studies. Blitz & Stark (1986, hereafter BS) reported the detection of low-level line wing emission in CO $J = 1 \rightarrow 0$ in the RMC, which they interpreted as originating in ubiquitous molecular interclump gas with very low average volume density ($n \approx 2$ cm^{-3}). Later, Williams, Blitz, & Stark (1995) favor a mostly atomic (H I) nature for the interclump gas with a density contrast of at least 40. Block, Dyson, & Madsen (1992) show that their observations of extended Hα emission enable them to optically probe the clump-interclump structure and claim that the interclump gas is partially ionized.

The subject of this Letter is to present new low-J ($J \leq 3$) CO observations in the RMC that suggest that the broad line wings reported by BS are due to dense gas with a low volume filling fraction rather than originating in a homogeneous, low-density, ubiquitous, molecular interclump component. A subsequent paper (Schneider et al. 1996) is devoted to discussing the extended mapping in the low-J CO and the 158 μm [C II] lines in the RMC.

2. OBSERVATIONS

We mapped the southeast part of the RMC in the $J = 3 \rightarrow 2$ and $2 \rightarrow 1$ lines of ^{12}CO and ^{13}CO with the Kölner Observatorium für Submillimeter-Astronomie (KOSMA) 3 m telescope. The data were obtained with cooled GaAs Schottky receivers ($T_{\rm rec}$ [230 GHz] = 400 K, $T_{\rm rec}$ [345 GHz] = 350 K) and an SIS receiver ($T_{\rm rec}$ [230 GHz] = 100 K). An acousto-optical spectrometer with a velocity resolution of 0.37 (0.25) km s^{-1} at 230 (345) GHz was used as back end. We mapped on an approximate beamwidth-sampled 2′ grid in $J = 2 \rightarrow 1$ and on a nearly fully sampled 40″ grid in $J = 3 \rightarrow 2$. All spectra are given in a T_R^* temperature scale; the efficiencies were derived by Jupiter continuum scans. Pointing was determined with Jupiter cross-scans and found to be accurate to within 10″. For the IRAM 30 m telescope observations, we selected four regions in the RMC (Fig. 1) to be observed in the ^{12}CO and ^{13}CO $2 \rightarrow 1$ transitions. The data were obtained with the facility SIS receivers ($T_{\rm rec}$ [single-sideband] around 120 K) and autocorrelators (velocity resolution 0.1 km s^{-1}). The standard IRAM chopper-wheel method was applied for calibration. The spectra were taken on an approximate beamwidth-sampled 15″ grid. Pointing was found to be accurate to within 3″. The significant pickup from a 170″ Gaussian error beam at 1.3 mm was removed by subtracting the appropriately smoothed and weighted KOSMA CO maps (Schneider & Stutzki 1994).

3. RESULTS

The Rosette Molecular Cloud is located at a distance of 1.6 kpc (Blitz & Thaddeus 1980) and is associated with an H II region illuminated by a central cluster of OB stars (NGC 2244). In their immediate vicinity, the stellar winds have

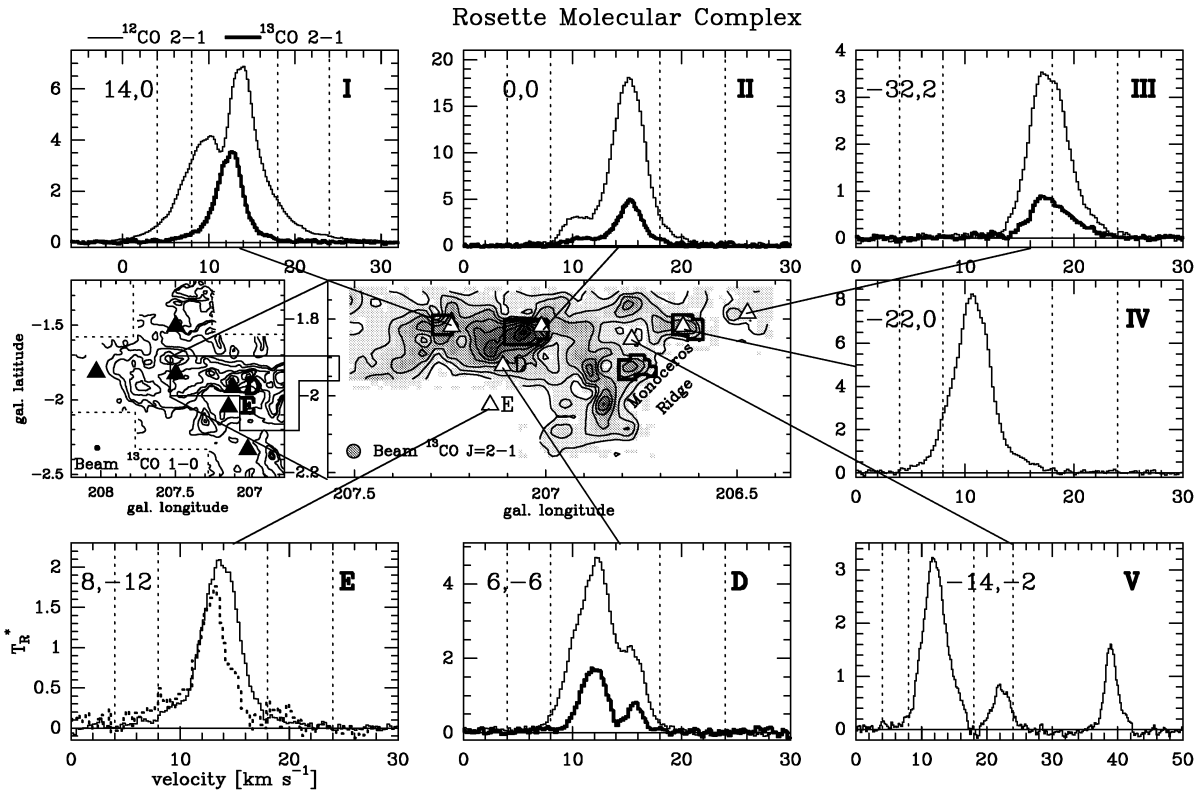

FIG. 1.—The extent of the velocity-integrated (4–24 km s^{-1}) KOSMA ^{13}CO $J = 2 \rightarrow 1$ map (*center middle panel*; gray-scale range starts at the 3 σ level) is indicated in the reproduced ^{13}CO $J = 1 \rightarrow 0$ map from BS (*left middle panel*). The four regions observed with the IRAM 30 m telescope are indicated in the KOSMA map. The locations where we have taken high-S/N spectra are marked, and the spectra are displayed in the surrounding boxes. The two velocity intervals v_1 (blue) and v_2 (red) of the CO emission ascribed to the "interclump gas" are denoted by dashed lines. The positions are given in arcminutes relative to the center position $l = 207\overset{\circ}{.}0154$, $b = -1\overset{\circ}{.}8228$ of the map. The thin (thick) line represents the ^{12}CO (^{13}CO) $J = 2 \rightarrow 1$ line. We reproduced the BS ^{12}CO $J = 1 \rightarrow 0$ spectrum (*dashed line*) at position E underlying the KOSMA ^{12}CO $J = 2 \rightarrow 1$ spectrum.

created a cavity. The southeast interface between the molecular cloud and the H II region is refered to as the "Monoceros Ridge." The RMC shows signs of active star formation, e.g., indicated by several embedded IR sources (Cox, Deharveng, & Leene 1990).

3.1. *Individual CO Line Profiles in the RMC*

BS reported the detection of line wings in the velocity intervals $v_1 = 4$–8 km s^{-1} (blue) and $v_2 = 18$–24 km s^{-1} (red) in ^{12}CO and ^{13}CO $J = 1 \rightarrow 0$ spectra at selected positions in the RMC, as well as in their positionally averaged spectra. Their ^{13}CO $J = 1 \rightarrow 0$ map with an angular resolution of 1.′8 is reproduced in Figure 1. The locations of their high signal-to-noise ratio (S/N) spectra [rms $\simeq$ 45(20) mK for ^{12}CO(^{13}CO) $J = 1 \rightarrow 0$], of which only spectrum E was published, are marked in the map. The KOSMA ^{13}CO $J = 2 \rightarrow 1$ map (Fig. 1) covers the highest intensity part of the cloud. We selected positions D and E from BS, together with five new positions for high-S/N measurements (rms 24–64 mK) in ^{12}CO and ^{13}CO $J = 2 \rightarrow 1$ with KOSMA, marked by I–V. It is immediately apparent that the spectra show a complex velocity structure with emission extending from -2 to 44 km s^{-1}, partially in overlapping line components. The main part of the molecular emission of the RMC is gathered in a velocity component around 12 km s^{-1}. This component is present throughout the cloud, with slightly position-dependent velocity shifts. The CO emission at position III, with a velocity around 18 km s^{-1}, arises from an isolated clump close to the H II region. Both the ^{12}CO and the ^{13}CO line profiles show enhanced emission at redshifted velocities. The CO line at position V shows several components well separated in velocity. The low-intensity ($T_R^* = 0.5$ K) ^{12}CO $J = 2 \rightarrow 1$ component in the velocity range 20–24 km s^{-1} has a FWHM of a few km s^{-1}, which is typical for the internal velocity dispersion of molecular clumps. It is not clear whether the component at 40 km s^{-1} is another high-velocity clump or an unrelated background source. The broad wing emission at position I, covering a velocity range from -2 to 28 km s^{-1}, is due to the outflow source AFGL 961 (Patel, Xie, & Goldsmith 1993). The spectra at position D and, in particular, position E reveal low-intensity wing emission in the velocity intervals $v_1 = 4$–8 km s^{-1} and $v_2 = 18$–24 km s^{-1}. The line profiles are similar to those of the CO $J = 1 \rightarrow 0$ wings reported by BS.

3.2. *Composite CO Spectra and Multiline Analysis*

Figure 2 compares ^{12}CO $J = 3 \rightarrow 2$, $2 \rightarrow 1$, and $1 \rightarrow 0$ spectra, positionally averaged over the same area. All spectra show wing emission in the velocity ranges $v_1 = 4$–8 km s^{-1} and $v_2 = 18$–24 km s^{-1}. The line shapes show slight differences due to different excitation conditions throughout the molecular complex. The high $3 \rightarrow 2/2 \rightarrow 1$ ratio in the blue wing might imply a higher density for the gas emitting this line component. A morphological analysis indicates that it originates predominantly in the outflow source near AFGL 961. The lower $3 \rightarrow 2/2 \rightarrow 1$ ratio in the red wing indicates lower densities for the gas emitting in this velocity range. This emission originates

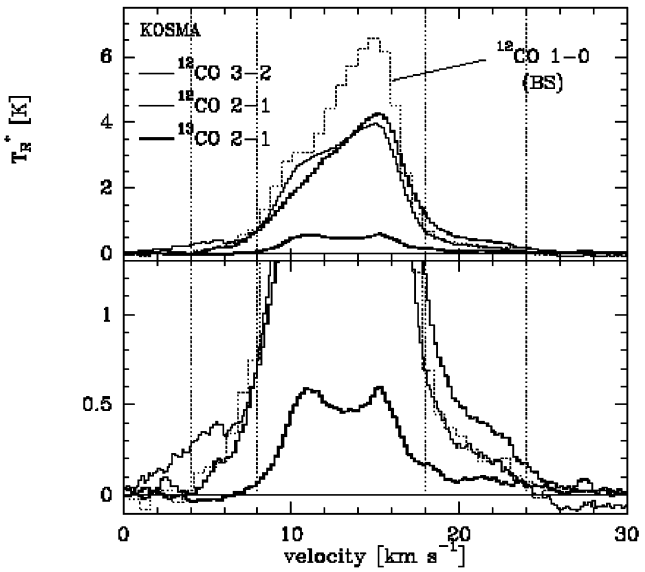

FIG. 2.—Spatially averaged isotopomeric CO spectra from BS and KOSMA observations. The KOSMA and BS maps are averaged over the same region (indicated by the KOSMA map in Fig. 1). The velocity intervals assigned to the molecular interclump gas emission are denoted by dashed lines. The lower panel is an enlargement of the line wings shown above.

mostly in individual clumps near the interface region as shown below.

For a multiline study, we selected positions E and II. At position E, the ratio of the velocity-integrated intensity between the ^{12}CO $J = 2 \rightarrow 1$ and $1 \rightarrow 0$ lines is 0.5 ± 0.1 (blue wing) 0.7 ± 0.1 (red wing), respectively. A correction for beam dilution of the KOSMA data (angular resolution 2′.2 compared with 1′.8 for the BS data) would slightly increase the line ratio. At position II, we took high-S/N ^{12}CO and ^{13}CO $J = 3 \rightarrow 2$ spectra in addition to the $J = 2 \rightarrow 1$ observations, displayed in Figure 3. The integrated line wing intensity ratio is approximately 1 between the $3 \rightarrow 2$ and $2 \rightarrow 1$ lines in each isotopomeric species and 5 for the ^{12}CO/^{13}CO line ratio.

Within a simple Escape Probability Radiative Transfer (EPRT) model (Stutzki & Winnewisser 1985), a $3 \rightarrow 2/2 \rightarrow 1$ line ratio of unity is possible either in the optically thin regime at a density of 3×10^4 cm^{-3} near the critical density in the transition region between background radiation and collisionally dominated excitation or over a wider range of densities in the optically thick and thermalized regime. The observed $3 \rightarrow 2/2 \rightarrow 1$ intensity ratio of unity is thus in contradiction to the excitation model proposed by Taylor et al. (1996) of very

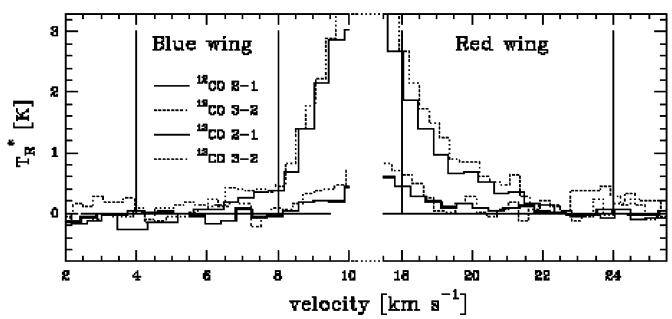

FIG. 3.—The blue and red wing section of the isotopomeric high-S/N CO line profiles at position II. The velocity intervals attributed to the interclump gas are marked with vertical lines.

low density, subthermally excited gas. In addition, the low intrinsic brightness of the lines in their model requires a beam-filling factor close to unity. The high optical depth (~10) at these excitation conditions, however, would then imply that the embedded clumps are not visible through this opaque interclump gas. The fact that a $3 \rightarrow 2/2 \rightarrow 1$ line ratio of ≈1 is observed for both ^{12}CO and ^{13}CO, and that, at the same time, the ^{12}CO/^{13}CO line ratio is ≈5, rules out that both ^{12}CO and ^{13}CO are optically thin.

The best fit to the observed line ratios within the EPRT model is obtained for densities between $10^{3.5}$ and $10^{4.5}$ cm^{-3}, and a ^{12}CO column density per velocity interval of 10^{17} cm^{-2} (1 km s^{-1})$^{-1}$ at a kinetic temperature around 30 K. Both the ^{12}CO $J = 3 \rightarrow 2$ and $2 \rightarrow 1$ lines are optically thick ($\tau > 10$). Because the brightness temperatures in this parameter space are significantly higher than the observed wing emission, a low area (and volume) filling factor for the emission and, hence, small scale clumpiness of the material are required. A density of 10^4 cm^{-3} and an H_2 column density of 4×10^{21} cm^2 (from the above CO column density and a standard CO abundance) for a single clump gives a clump diameter of 0.13 pc. In the KOSMA 120″ beam, the area filling factor is approximately 0.02. One should note, however, that the model does not give a very good fit to all line ratios simultaneously; in particular, the ^{12}CO/^{13}CO line ratio of 5 is difficult to obtain, even in the regime of moderately dense gas and optically thick ^{12}CO emission. The situation is similar to the one found in other sources (e.g., Orion B; Kramer, Stutzki, & Winnewisser 1996). A natural explanation for this discrepancy might be an inside/out temperature gradient, e.g., due to external heating of the clumps by the ambient UV field, so that the lower optical depth ^{13}CO emission originates in lower temperature material deeper in the molecular clump.

4. THE ORIGIN OF THE LINE WINGS

With these results in mind, we propose that the wing emission originates from the superposition of individual small, dense, high-velocity clumps and from embedded outflow sources. Thus, the observed line wings do not provide evidence for a ubiquitous, molecular, low-density interclump gas.

The blue wing (velocity interval $v_1 = 4–8$ km s^{-1}) CO emission is primarily due to the outflow source AFGL 961. Spectrum I in Figure 1 exhibits strong line wings in this velocity range. The spatial extent of the outflow, estimated from the KOSMA ^{12}CO $J = 3 \rightarrow 2$ map, is at least 3′ × 3′.4. In addition, the line wing emission from clumps with a line-center velocity lower than 12 km s^{-1} contributes to the blue wing. Such clumps are found, e.g., at the H II region/molecular cloud border (spectrum IV in Fig. 1). Thus, a positionally averaged spectrum, including the regions of the outflow source and the low-velocity clumps, shows "wing emission" in the velocity range 4–8 km s^{-1}. Consequently, the integrated intensity of the blue wing emission is reduced by a factor 2 if the spectra of these regions are excluded for averaging. This suggests that additional clumps or outflows hidden in the extended low-resolution map contribute to the wings. One such outflow source was recently detected near position II (Schneider et. al 1996).

The red wing (velocity interval $v_2 = 18–24$ km s^{-1}) emission originates mainly from the superposition of distinct clumps. Figure 4 shows a contour plot of the KOSMA ^{13}CO $J = 2 \rightarrow 1$ emission in this velocity range. A number of clumps in the

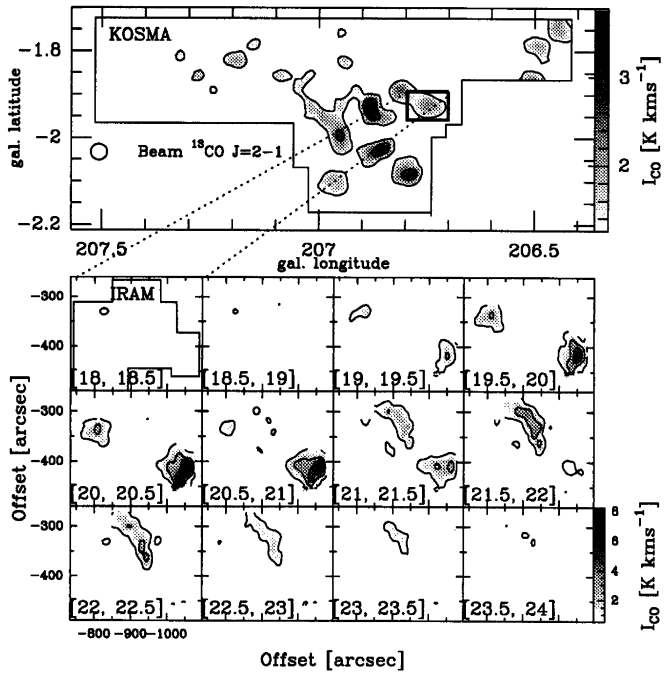

FIG. 4.—The KOSMA ^{13}CO $J = 2 \rightarrow 1$ map, integrated over the red velocity interval v_2 (*top panel*), shows a number of clumps close to and in some distance from the H II region (gray-scale range starts at 3 σ). One of the clumps in the Monoceros Ridge was mapped in ^{13}CO $J = 2 \rightarrow 1$ with IRAM, revealing the spatial and velocity substructure in the velocity range v_2.

"Monoceros Ridge" region with an integrated intensity well above the 3 σ level are clearly identified. The higher velocity of these clumps, compared with the average velocity of about 12 km s^{-1} for the RMC, could result from an outward acceleration of the gas due to the interaction with the H II region and the embedded IR sources. One of the clumps, located in the immediate vicinity of the H II region, was observed with the IRAM 30 m telescope (Fig. 4). Channel maps of these high spatial resolution ^{13}CO $J = 2 \rightarrow 1$ data confirm the small-scale substructure of the clump.

5. CONCLUSIONS

Our observations show broad CO wing emission in the positionally averaged low-J CO spectra as well as in individual high-S/N spectra in the RMC. Analysis of the excitation conditions suggests that the wing emission originates in gas with densities comparable to those of the bulk material ($\geq 10^4$ cm^{-3}). High spatial resolution maps of selected regions confirm that, at least there, the wings are due to a combination of beam-diluted emission from individual clumps with significant small-scale substructure and embedded outflow sources. There is thus no need to invoke the presence of a ubiquitous low-density molecular interclump gas to explain the low-level wing emission. Applying the results of a simple EPRT multiline analysis implies a clump internal pressure that is higher than the average for the entire complex. Accordingly, the presence of small high-density clumps in this environment is not straightforward to understand. Broad wing emission apparently is a general property of molecular clouds (Falgarone & Phillips 1990), and revealing the nature of this emission is essential for understanding the evolution of the clouds. The results presented favor a picture of small unresolved clumps, but further high-resolution, high-sensitivity observations in the $3 \rightarrow 2$ and $2 \rightarrow 1$ lines in those regions of the RMC, where the effects of external heating are likely to be minimal, are required to resolve the problems posed by the necessity of pressure equilibrium.

We thank J. Williams for preparing the positionally averaged CO $J = 1 \rightarrow 0$ spectra from the BS data set. The KOSMA 3 m telescope is operated by the University of Cologne and supported by the Deutsche Forschungsgemeinschaft through grant SFB-301, as well as special funding from the Land Nordrhein-Westfalen. The Observatory is administered by the Internationale Stiftung Hochalpine Forschungsstationen Jungfraujoch und Gornergrat, Bern.

REFERENCES

Bertoldi, F., & McKee, C. F. 1992, ApJ, 395, 140
Blitz, L., & Stark, A. 1986, ApJ, 300, L89 (BS)
Blitz, L., & Thaddeus, P. 1980, ApJ, 241, 676
Block, D., Dyson, J., & Madsen, C. 1992, ApJ, 390, L13
Cox, P., Deharveng, L., & Leene, A. 1990, A&A, 230, 181
Falgarone, E., & Phillips, T. 1990, ApJ, 359, 344
Kramer, C., Stutzki, J., & Winnewisser, G. 1996, A&A, 307, 915
Patel, N., Xie, T., & Goldsmith, P. 1993, ApJ, 413, 593
Perault, M., Falgarone, E., & Puget, J. L. 1985, A&A, 152, 371
Schneider, N., & Stutzki, J. 1994, IRAM Newsletter No. 15
Schneider, N., et al. 1996, in preparation
Stutzki, J. 1993, Rev. Mod. Astron., 6, 209
Stutzki, J., & Güsten, R. 1990, ApJ, 356, L63
Stutzki, J., & Winnewisser, G. 1985, A&A, 144, 13
Stutzki, J., Stacey, G. J., Genzel, R., Harris, A. I., Jaffe, D. T., & Lugten, J. B. 1988, ApJ, 332, 379
Taylor, S. D., et al. 1996, ApJ, submitted
Williams, J. A., Blitz, L., & Stark, A. A. 1995, ApJ, 451, 252 OK?